Influence of Cr substitution on the reversibility of the magnetocaloric effect in Ni-Cr-Mn-In Heusler alloys

C. Salazar-Mejía,[1,*] P. Devi,[2,3,4] S. Singh,[2,5] C. Felser,[2] and J. Wosnitza[1,6]

[1]*Hochfeld-Magnetlabor Dresden (HLD-EMFL) and Würzburg-Dresden Cluster of Excellence ct.qmat, Helmholtz-Zentrum Dresden-Rossendorf, 01328 Dresden, Germany*

[2]*Max Planck Institute for Chemical Physics of Solids, 01187 Dresden, Germany*

[3]*Center for Quantum Nanoscience, Institute for Basic Science (IBS), Seoul 03760, Republic of Korea*

[4]*Department of Physics, Ewha Womans University, Seoul 03760, Republic of Korea*

[5]*School of Materials Science and Technology, Indian Institute of Technology (BHU), Varanasi-221005, India*

[6]*Institut für Festkörper- und Materialphysik, TU Dresden, 01062 Dresden, Germany*

(Received 28 May 2021; revised 19 August 2021; accepted 29 September 2021; published 13 October 2021)

We present the effect of substitution-induced pressure on the reversibility of the magnetocaloric effect (MCE) in $Ni_2Cr_xMn_{1.4-x}In_{0.6}$ ($x = 0.1, 0.2, 0.3$) alloys, through characterization in pulsed magnetic fields. We measured the adiabatic temperature change ΔT_{ad} directly during applied magnetic field pulses of 2 and 6 T. We paid special attention to the reversibility of ΔT_{ad}. The substitution of Mn by Cr in $Ni_2Mn_{1.4}In_{0.6}$ leads to a negative pressure, as evidence by the increase of the lattice parameters, which shifts the martensitic transition towards lower temperatures and enhances the ferromagnetism of the martensite phase. We found a large value of $\Delta T_{ad} = -7$ K at $T = 270$ K for the sample with $x = 0.1$ for a field change of 6 T. We discuss the reversibility of the MCE in these alloys in terms of the Clausius-Clapeyron equation.

DOI: 10.1103/PhysRevMaterials.5.104406

I. INTRODUCTION

Ni-Mn-based shape-memory Heusler alloys are well known for their fascinating multifunctional properties such as giant magnetocaloric effect (MCE) [1,2], giant barocaloric effect [3], field-induced shape-memory effect [4], and magnetic superelasticity [5]. These properties are closely related to the first-order martensitic transition appearing in these alloys. The MCE manifests itself as a change in the temperature of a material by applying magnetic field and can be quantified in terms of isothermal entropy and adiabatic temperature change [1,5–7]. Heusler alloys exhibit large magnetocaloric effects, however, missing reversibility is an issue that has been extensively studied and discussed [7–13].

Our previous reports show a detailed study of the MCE in pulsed magnetic fields for the shape-memory Heusler alloy $Ni_2Mn_{1.4}In_{0.6}$ [8]. This alloy exhibits a conventional MCE of $\Delta T_{ad} = 5$ K around 315 K (the Curie temperature) and a large inverse MCE of $\Delta T_{ad} = -7$ K at 250 K (martensitic transition) under a magnetic field change of 6 T [8]. However, the inverse MCE is irreversible. Recently we have shown that reversible MCEs can be obtained in Ni-Mn-based shape-memory Heusler alloys as a result of improving the compatibility between the austenite and martensite crystal structures [7,9]. We have also reported on the effect of externally applied pressure on the reversibility of the MCE in Ni-Cu-Mn-In Heusler alloys [14]. Another strategy to improve the reversibility of the MCE in the Ni-Mn-based family of alloys is a tailored substitution of the transition elements and, in this way, reducing or increasing the chemically induced pressure without avoiding the first-order phase transition that leads to the large inverse MCE.

Predictions from Monte Carlo and *ab initio* calculations show that Cr substitution in Ni-Mn-In-based Heusler alloys could lead to a large inverse MCE due to a pronounced magnetization jump at the martensitic transition. This is due to the appearance of a paramagnetic or antiferromagnetic gap at temperatures below the structural transformation [15,16]. *Ab initio* calculations reported in Ref. [16] indicate $Ni_2Cr_{0.25}Mn_{1.25}In_{0.5}$ as the most suitable composition in Ni-Cr-Mn-In-based alloys for application in magnetic refrigeration. The calculations predict that the martensite phase of this alloy is ferrimagnetic while the austenite is ferromagnetic and, consequently, a large magnetization jump should occur at the structural transition from martensite to austenite [16]. Different attempts to substitute Cr in the Ni-Mn-In alloys have been reported in literature [17–20]. Controversial results have been reported, for instance, the unusual effect of Cr to increase the martensitic transition temperature despite the concomitant decrease of the valence electron concentration per atom, e/a [18,20]. Sanchez-Alarcos *et al.* [21] have pointed out a very low solubility of Cr in Ni-Mn-In, which leads to the appearance of a Cr-rich second phase, even for quite low Cr concentrations. Pandey *et al.* also reported that substitution of Cr for Ni in $Ni_{50-x}Cr_xMn_{37}In_{13}$ enhances the MCE [17]. Thus, the effect of Cr doping in the Ni-Mn-In-based alloys, in terms of composition stability, phase-transition behavior, and MCE is not yet clear from the experimental point of view.

*c.salazar-mejia@hzdr.de

 ©2021 American Physical Society

Moreover, a direct measurement of the adiabatic temperature change and its reversibility, which is important for the technological application of these alloys, has not been addressed in the literature, so far.

In the present study we have successfully prepared single-phase shape-memory Heusler alloys of the series $Ni_2Cr_xMn_{1.4-x}In_{0.6}$, with $x = 0.1$, 0.2, and 0.3. We have investigated the magnetic and magnetocaloric properties in view of possible applications. Substitution of the low atomic number transition element Cr for Mn tunes the structural and ferromagnetic transition towards lower temperatures. All samples show a structural transition in the temperature range between 200 and 300 K, below the Curie temperature T_C. We have characterized the magnetocaloric effect (specifically, the adiabatic temperature change ΔT_{ad}) due to the martensitic magnetostructural transformation in these alloys, under applied magnetic-field pulses of 2 and 6 T. All of these shape-memory Heusler alloys exhibit a large inverse MCE (temperature decrease under field application) due to the field-induced martensitic transition and a conventional MCE (temperature increase under field application) associated with the ferromagnetic transition.

II. EXPERIMENTAL DETAILS

We prepared polycrystalline ingots of $Ni_2Cr_xMn_{1.4-x}In_{0.6}$ ($x = 0.1$, 0.2, and 0.3) by induction melting from high-purity commercially available elements of Ni, Cr, Mn, and In in an Ar atmosphere with an overall mass loss of less than 0.02 wt. %. A two-step process was employed for each sample. First, a premelt of Ni-Cr was prepared. According to the phase diagram, Ni and Cr react very well with each other and form a stable phase. In the next step, when the premelt is heated, it absorbs the Mn and In pieces that we added to the melt. As a result, after the Mn and In are absorbed, evaporation of the complete phase, not the single elements, takes place. All samples were melted four times on each side to ensure homogeneity. The melted ingots were then annealed at 900 °C for three days and subsequently quenched into an ice water mixture.

We performed structural characterization at room temperature (RT) with powder x-ray diffraction (XRD) using a Huber G670 camera (Guinier technique, $\lambda = 1.54056$ Å, Cu-$K\alpha$ radiation). Prior to doing XRD, all samples were ground into powder and annealed at 700 °C, which reduces the stress generated during grinding [14,22]. Scanning electron microscopy (SEM) and energy dispersive x ray (EDX) were used to study the composition. Prior to SEM and EDX analyzes, small pieces were cut from the samples with a diamond saw. To prepare a smooth surface, the pieces were embedded in epoxy-resin blocks and polished.

We carried out magnetization measurements in a Physical Property Measurement System (PPMS, Quantum Design). Direct measurements of ΔT_{ad} were performed in a home-built experimental setup in pulsed magnetic fields at the Dresden High Magnetic Field Laboratory (HLD). Short pulse durations (20–50 ms) allow for adiabatic conditions, making possible to measure ΔT_{ad} without heat losses [8].

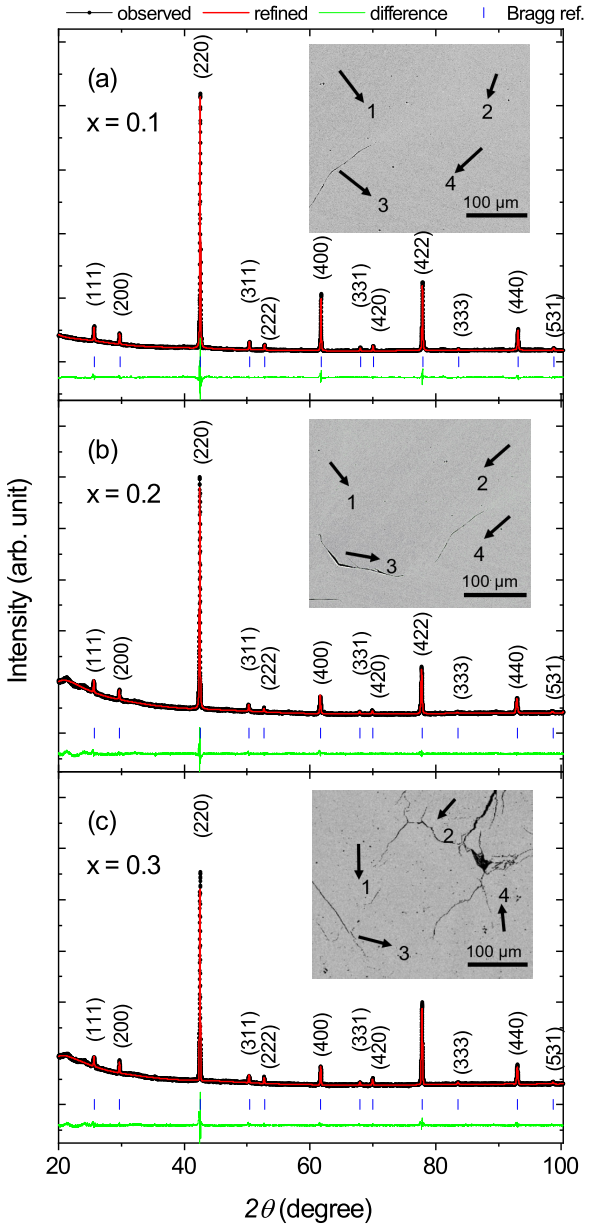

FIG. 1. XRD results of the $Ni_2Cr_xMn_{1.4-x}In_{0.6}$ samples at room temperature, for (a) $x = 0.1$, (b) $x = 0.2$, and (c) $x = 0.3$. Calculated diffractograms and differences to the observed ones are also shown for each sample. The positions of the Bragg peaks are indicated. The inset shows room-temperature SEM images of each alloy. Black arrows indicate the spots where the composition was analyzed in detail.

III. RESULTS AND DISCUSSION

The observed and calculated ($L2_1$ cubic structure, space group $Fm\bar{3}m$) XRD patterns at RT for all samples are presented in Fig. 1. The observed Bragg reflections (for all samples) are accounted very well by the cubic $L2_1$ crystal structure, which reveals the phase purity of the samples. The refined lattice parameters are $a = 6.005 \pm 0.002$ Å for $x = 0.1$, $a = 6.012 \pm 0.004$ Å for $x = 0.2$, and $a = 6.037 \pm 0.001$ Å for $x = 0.3$, which shows that the Cr substitution induces a negative pressure in the material. It is worth to

TABLE I. Element concentration determined by EDX at four different spots on the samples, as indicated in the insets of Fig. 1.

Alloy	Spot	Ni (at %)	Mn (at %)	Cr (at %)	In (at %)
	1	47.55	31.97	1.98	18.49
0.1	2	49.99	30.44	2.19	17.38
	3	49.78	30.74	2.50	16.99
	4	48.94	30.05	2.55	18.45
	1	48.99	29.57	5.65	15.80
0.2	2	44.17	30.77	7.48	17.58
	3	47.54	29.84	4.97	17.65
	4	47.50	29.82	6.23	16.45
	1	47.58	28.03	5.65	18.74
0.3	2	47.54	28.85	5.00	18.61
	3	48.87	27.87	6.52	16.74
	4	47.51	27.73	7.12	17.64

mention that a sample with higher Cr concentration, $x = 0.4$, was also prepared. However, the presence of secondary phases was observed (see the Supplemental Material for details [23]). The insets of Fig. 1 show SEM images taken for the samples, which reflect homogeneous compositions without the presence of secondary phases. EDX analysis was performed at four different locations on each sample, marked in the figure. The element concentration at the four spots shows a homogeneous distribution through the sample, within the limits of the EDX technique (Table I and the Supplemental Material [23]). We note that from EDX results, it seems that the Cr content between sample $x = 0.2$ and $x = 0.3$ is quite similar. However, as we will show next, there is a consistent change of the transition temperatures and magnetic properties for these samples that indeed indicates a real change in Cr substitution. As $x = 0.3$ is a critical composition (for higher Cr values secondary phases appear), it is possible that some disorder is already present in the sample that alters the EDX results but it is just too small to detect. For the discussion we will refer to the nominal x value for simplicity.

Figures 2(a)–2(c) show temperature-dependent magnetization data $M(T)$ for all samples, at 0.01 (right axis), 2, and 6 T (left axis), recorded upon cooling (closed symbols) and subsequent heating (open symbols). All samples undergo a first-order martensitic transition at temperatures T_M below the ferromagnetic ordering temperature T_C. The hysteresis width observed around the first-order martensitic transition in these alloys is approximately 10 K or larger. For the alloy with $x = 0.1$, the martensitic transition takes place on cooling at $T_M = 270$ K from a ferromagnetic austenite phase ($T_C = 312.5$ K) to a weakly magnetic martensite that orders ferromagnetically at around 200 K. In this weakly magnetic martensitic phase both antiferromagnetic and ferromagnetic interactions are present [24]. With Cr substitution, the ferromagnetism of the martensitic phase is enhanced over the antiferromagnetism and the structural transition takes place between two ferromagnetic phases. In the other two alloys, $x = 0.2$ and $x = 0.3$, the martensitic transition takes place between the ferromagnetic austenite and the ferromagnetic martensite state. The substitution of Mn by Cr shifts the martensitic transition towards lower temperatures and enhances the ferromagnetic interactions in the martensite phase, as also reported for

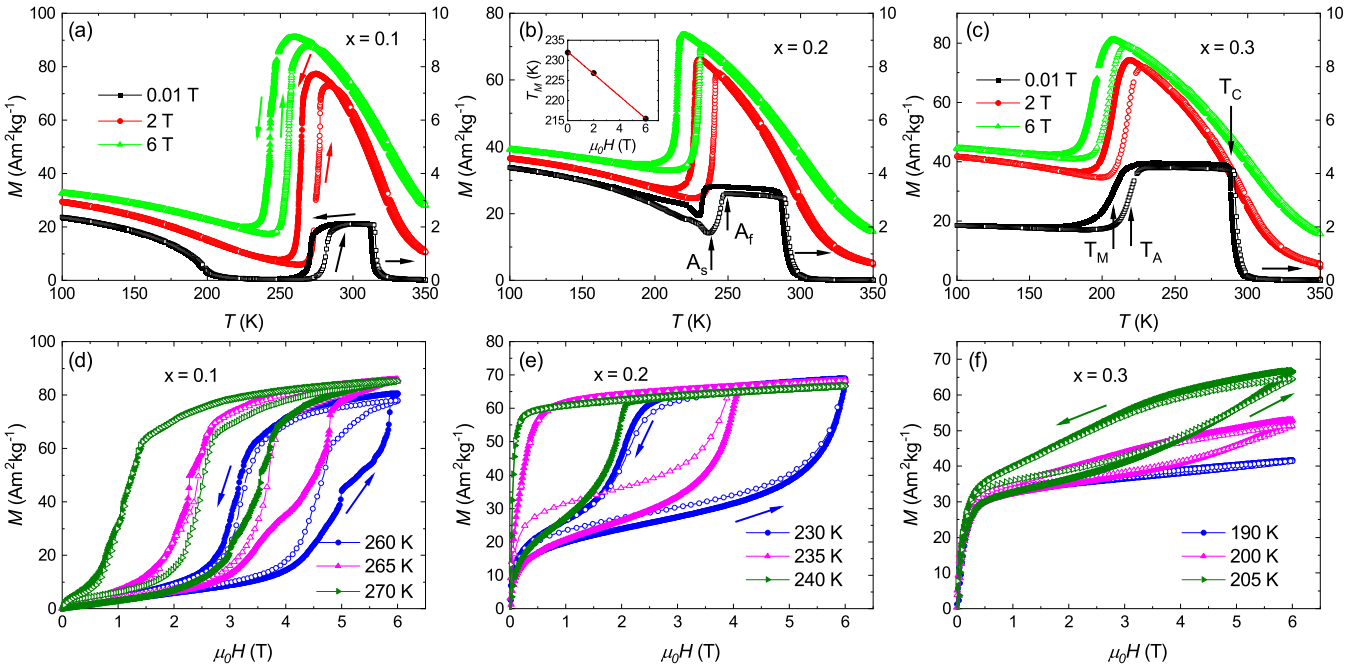

FIG. 2. Temperature dependence of the magnetization of $Ni_2Cr_xMn_{1.4-x}In_{0.6}$ for (a) $x = 0.1$, (b) $x = 0.2$, and (c) $x = 0.3$ at magnetic fields of 0.01, 2, and 6 T. The right axes show the scale for the 0.01 T data. Closed symbols indicate measurements upon cooling and open symbols those recorded during heating. The inset of (b) shows the variation of T_M with field and the red line is the linear fit to the data. Field-dependent magnetization at different temperatures for (d) $x = 0.1$, (e) $x = 0.2$, and (f) $x = 0.3$. Closed symbols indicate first measurements after reaching the target temperature following the discontinuous heating protocol (see text) and open symbols indicate repeated measurements without heating or cooling in between.

TABLE II. Transition temperatures of the $Ni_2Cr_xMn_{1.4-x}In_{0.6}$ alloys. For the definition of T_C, T_A, T_M see Fig. 2(c).

x	T_C (K)	T_M (K)	T_A (K)	dT_M/dH (K/T)
0.1	312.5	270	281.5	−4.6
0.2	288	232	245	−2.8
0.3	288.5	207.8	219.8	−2.5

Ni-Mn-Cr-Sb alloys [25]. We have measured the magnetization at 10 K for all samples and the magnetic moment of the martensite phase increases with Cr substitution (see the Supplemental Material [23]). Consequently, the magnetization difference between the martensite and austenite phases decreases.

Table II gathers the characteristic transition temperatures of the samples, determined as the inflection points of the $M(T)$ curves. T_C is the Curie temperature in the austenite, T_M is the martensitic transition temperature upon cooling, and T_A indicates the reverse martensitic transition, upon heating, as it is marked in Fig. 2(c). Additionally, in Fig. 2(b) we have also marked the austenite start temperature A_s and the austenite finish temperature A_f. For all samples, T_M decreases linearly with field, as shown in the inset of Fig. 2(b) for $x = 0.2$. As has been seen in other Ni-Mn-Z-based Heulser alloys (with Z = In, Sb, Sn), the magnetic field shifts the structural transition toward lower temperatures as the austenite phase is stabilized. dT_M/dH is extracted as the slope of the linear fit of T_M versus field [inset of Fig. 2(b)] and quantifies the sensitivity of the martensitic transition to the magnetic field. This value for the Cr-doped alloys is rather weak compared with the Ni-Mn-In parent compound ($dT_M/dH \approx -7$ K/T [8]) but still higher than for other Ni-Mn-based Heusler alloys [26]. According to the Clausius-Clapeyron equation, $dT_M/dH \cong \mu_0 \Delta M/\Delta S$, the sensitivity of the martensitic transition to the field not only depends on the magnetization jump at the transition ΔM but on the transition entropy change ΔS. Actually, ΔS has a stronger influence on dT_M/dH as ΔM [27]. It has been shown as well, that in Ni-Mn-Z (Z = In, Sn, Sb) Heusler alloys the transition entropy strongly depends on the distance between the Curie temperature and the martensitic transition temperature $|T_C - T_M|$. The entropy change at the transition decreases with the increase of $|T_C - T_M|$ [28–31]. With Cr substitution in the $Ni_2Cr_xMn_{1.4-x}In_{0.6}$ series, the distance $|T_C - T_M|$ increases, as can be seen in Table II. Therefore, we expect that ΔS decreases with Cr. Consequently, we observe a decrease of dT_M/dH through the series of samples.

Figures 2(d)–2(f) present magnetic-field-dependent magnetization $M(H)$ up to 6 T for all samples, recorded at selected temperatures around the martensitic transformation. Two measurements were performed at each temperature in order to check the reproducibility of the first-order induced transition. The closed symbols are data measured after reaching the target temperature T_i following the discontinuous heating protocol (DHP) described below and the open symbols shows the data subsequently measured without heating or cooling in between. In the DHP the sample was first heated up to 350 K (fully austenite phase), followed by cooling down to 200 K (fully martensite phase), and then reaching T_i upon heating.

We choose the selected temperatures to lie below T_A, meaning that the sample is in the martensite state, before applying the magnetic field. Therefore, the austenite state is induced due to the magnetic field. Interestingly, different results are obtained for the samples. In the case of $x = 0.1$, 6 T is sufficient to induce a complete reverse martensitic transition at the selected temperatures, while for $x = 0.2$ and 0.3 the transition is not complete. However, for the latter compounds the magnetization behavior is more reproducible, i.e., the repeated hysteresis loops lie close to the first ones. In the case of the alloy with $x = 0.1$, there is a large difference between the first and the following data for the up-sweep branch. When T_i is reached following the DHP, the field-induced transition is quite broad, for instance, at $T_i = 265$ K the transition starts around 3 T and finishes around 5 T while, for the following cycle, it finishes around 4 T. Additionally, the magnetization does not increase monotonously but shows steplike features. For the down sweep (austenite to martensite transition), both curves follow the same path. These steplike features are related to the way the austenite phase grows into the martensite phase, or, in other words, the annihilation of the martensite [32] and it is observed every time T_i is reached following the DHP.

From the $M(H)$ curves we further observe that the martensite state of the alloys with $x = 0.2$ and $x = 0.3$ is ferromagnetic at temperatures close to T_A.

We have measured the adiabatic temperature change ΔT_{ad} during magnetic field pulses of 2 and 6 T. First pulses were obtained following the DHP and follow-up pulses, without heating or cooling in between, were applied at selected temperatures. First, we will discuss the results for 6 T pulses.

Figure 3 shows time-dependent data of ΔT_{ad} at selected temperatures, together with the time-dependent magnetic field. At temperatures T_i above T_A, close to T_C, when the samples show a conventional MCE, ΔT_{ad} follows closely the applied magnetic field change with only little delay (less than 1 ms) due to experimental artifacts (black curve in Fig. 3). For lower T_i, however, when the inverse MCE appears, ΔT_{ad} follows the field change only with large delay and strongly disturbed time-dependent profiles. Specifically, for the case of $x = 0.1$, $T_i = 265$ K [blue curve in Fig. 3(a)] lies below the austenite start temperature $A_s = 275$ K, and, as it can be seen in the $M(H)$ curves showed in Fig. 2(d), at this temperature the transition from martensite to austenite is induced and completed (i.e., the sample transforms back when the field is reduced). When the measurement is repeated [light blue curve in Fig. 3(a)], without heating or cooling the sample in between, a similar result is obtained, however, smaller effects are observed. This is reflected as well on the magnetization data. The $M(H)$ curves in Figs. 2(d)–2(f) can help to understand the ΔT_{ad} results, but no one-to-one comparison should be made, as the pulse-fields measurements are performed under adiabatic conditions while the static-field $M(H)$ are done under isothermal conditions [33].

At $T_i = 275$ K and $x = 0.1$ [red in Fig. 3(a)], the MCE is highly irreversible due to the fact of being in the middle of the hysteretic region. After the pulse, a large fraction of the sample remains in the austenite and does not transform back to

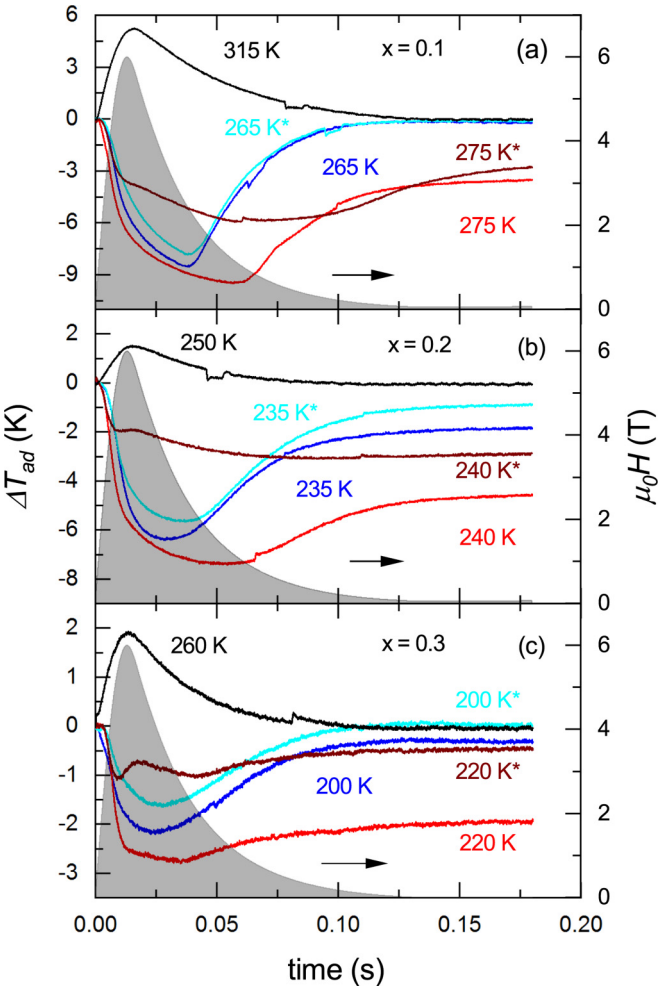

FIG. 3. Time-dependent $\Delta T_{\rm ad}$ at selected T_i for (a) $x = 0.1$, (b) $x = 0.2$, and (c) $x = 0.3$ during 6 T magnetic field pulses. The temperatures marked with $*$ indicate repeated pulses, while the DHP was followed to reach T_i for the other results. The right axes shows the time-dependent magnetic field.

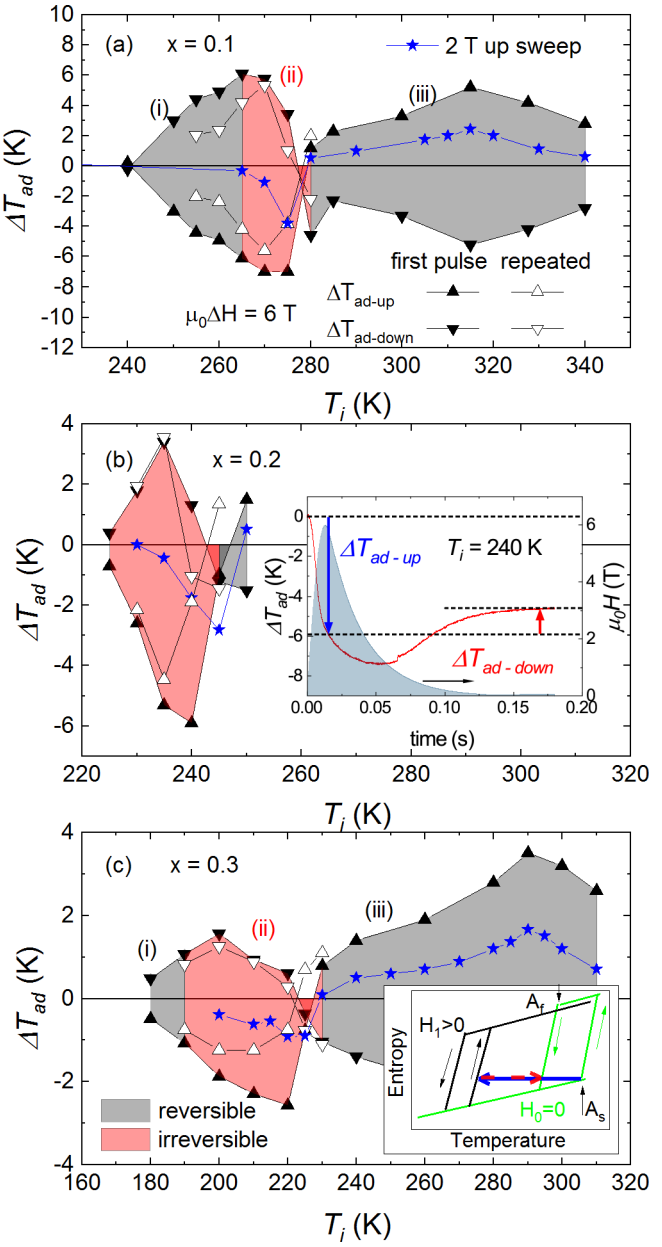

FIG. 4. $\Delta T_{\rm ad}$ obtained for up and down sweeps using 6 T pulses for (a) $x = 0.1$, (b) $x = 0.2$, and (c) $x = 0.3$. Results for 2 T pulses (up-sweep) and repeated pulses in the hysteresis region are also included. The inset of (b) shows time-dependent $\Delta T_{\rm ad}$ at $T_i = 240$ K for $x = 0.2$ and the time-dependent magnetic field, together with the illustration of how $\Delta T_{\rm ad\text{-}up}$ and $\Delta T_{\rm ad\text{-}down}$ are extracted. The inset of (c) shows a schematic drawing of the MCE if measured for up-sweep (blue arrow) or down-sweep (red arrow). See text for details.

the martensite phase. When a second pulse is given [dark red in Fig. 3(a)], the result is a mixture of inverse MCE, due to the transformation from martensite to austenite and conventional MCE caused by the austenite already present in the sample after the first pulse. A similar behavior is observed for the other two samples. The results in blue are for a $T_i < A_s$ and red ones are for $A_s < T_i < A_f$, where A_f is the austenite finish temperature [see Fig. 2(b)]. It is worth to point out that, while there is a large difference of the $M(H)$ results for the different samples [Fig. 2(d)–2(f)], the $\Delta T_{\rm ad}$ results are quite similar for the three samples, with the main difference being the net MCE measured.

Figure 4 shows the adiabatic temperature changes as a function of the starting temperature T_i for all samples. These values are extracted from the time-dependent data as illustrated in the inset of Fig. 4(b). In order to study the reversibility of the effect, i.e., to study whether the initial temperature is recovered after field removal, we extract $\Delta T_{\rm ad}$ for field up- and down-sweeps [34]. From the comparison of the MCE obtained under a first pulse (closed symbols in Fig. 4) and the values reached under a follow-up pulse (open symbols), we study the reproducibility of the effect, i.e., whether the same results are obtained after repeating the pulse.

Analyzing the data in Fig. 4, we can highlight three regions in the MCE for all samples. Region (i): the martensite to austenite transition is induced during the 6 T pulses, and after field removal the sample transforms completely back to the martensite phase, recovering T_i with $|\Delta T_{\rm ad\text{-}up}| = |\Delta T_{\rm ad\text{-}down}|$.

Region (ii): the martensitic transition is fully (or partially) induced during the up-sweep, but when removing the field only part of the sample transforms back to the martensite and $|\Delta T_{\text{ad-up}}| > |\Delta T_{\text{ad-down}}|$. The MCE is irreversible in this region (red in Fig. 4). Finally, conventional MCE is observed in region (iii), where $|\Delta T_{\text{ad-up}}| = |\Delta T_{\text{ad-down}}|$. The MCE is not reproducible in regions (i) and (ii), as for a second pulse a reduced MCE is recorded for all samples. However, it is interesting to notice that for $x = 0.2$ and $x = 0.3$ the MCE obtained after field removal ($\Delta T_{\text{ad-down}}$) is almost reproducible, while $\Delta T_{\text{ad-up}}$ differs largely between a first and a second pulse.

About the effect of the Cr substitution on the values of the MCE, we see that the sample with $x = 0.1$ reaches the largest temperature change $\Delta T_{\text{ad-up}} = -7$ K for $T_i = 270$ K (similar to the parent compound [8]). This maximum $\Delta T_{\text{ad-up}}$ reduces to about -6 K for $x = 0.2$ and -2.5 K for $x = 0.3$. For the latter alloy, it is important to note that the field of 6 T is not sufficient for a complete martensite to austenite transformation [see Fig. 2(f)]. For a second field pulse without thermal cycling the samples (open symbols in Fig. 4), only $\Delta T_{\text{ad-up}} = -5.6$ K is reached for $x = 0.1$.

In Fig. 4 we also show $\Delta T_{\text{ad-up}}$ results for 2 T pulses (star symbols). As expected, the MCE is lower due to the lower field and expands over a smaller temperature region below T_A in comparison with the results for 6 T pulses. For the 2 T pulses, the sample with $x = 0.1$ exhibits the largest temperature change of -4 K at around 275 K. This MCE decreases with Cr substitution to a value of -1 K at 224 K for the sample with $x = 0.3$. It is important to note that 2 T is not sufficient for a complete transition in most of the temperature region investigated.

In general, the MCE decreases with Cr substitution. This has three origins: (i) 2 and 6 T are not sufficient to induce a complete martensitic transition for most of the temperature region for the $x = 0.2$ and $x = 0.3$ alloys; (ii) the magnetization difference between the martensite and austenite phases decreases with Cr substitution; and (iii) $|T_C - T_M|$ increases with Cr substitution which leads to a reduction of $|\Delta T_{\text{ad}}|$ due to the contradictory role of the magnetic and structural contributions to the MCE in Ni_2Mn-based Heusler alloys [30,31]. At the same time, the increase of $|T_C - T_M|$ leads to a decrease in the sensitivity of the transition to the field dT_M/dH, as previously discussed. This is the reason why higher fields are needed to induce a complete martensitic transition as the Cr content increases.

The region of irreversibility of the MCE also increases with Cr substitution. With the help of the schematic drawing presented in the inset of Fig. 4(c) we can understand why the irreversibility increases. The drawing shows the entropy curves at $H_0 = 0$ and $H_1 > 0$ for the case of a martensitic transition in Heusler alloys. We have considered also the hysteresis of the transition [34,35]. The reversibility of ΔT_{ad} has its origins on the relation between the thermal hysteresis of the first-order martensitic transition and the sensitivity of the transition to the magnetic field (dT_M/dH), i.e., how much the entropy curve for $H_1 > 0$ is shifted to the left in the schematic drawing of Fig. 4(c). When dT_M/dH is weak, as it is the case for $x = 0.2$ and 0.3, a moderated magnetic field of 2 and 6 T is not sufficient to induced a complete martensite to austenite transition. On the up-sweep only some of the sample transforms from martensite to austenite and $|\Delta T_{\text{ad-up}}|$ is obtained [blue arrow in the inset of Fig. 4(c)]. The state after the up-sweep is a mixture of martensite and austenite phases. When the field is removed, the portion of the austenite that transforms back to martensite is limited by the hysteresis of the transition and the obtained $|\Delta T_{\text{ad-down}}|$ is smaller, as indicated by the red arrow. As previously mentioned, as Cr increases and the martensitic transition shifts toward lower temperatures, the distance $|T_C - T_M|$ increases. This leads to a decrease of the transition entropy ΔS, and, from the Clausius-Clapeyron equation $dT_M/dH \cong \mu_0 \Delta M/\Delta S$, dT_M/dH also decreases with Cr substitution, leading then to a larger irreversibility of the MCE.

As mentioned in the Introduction, *ab initio* calculations predict the $Ni_2Cr_{0.25}Mn_{1.25}In_{0.5}$ alloy as being the most suitable Ni-Cr-Mn-In-based alloy for application in magnetic refrigeration [16]. The alloys with $x = 0.2$ and $x = 0.3$ are close to this composition, however, calculations have predicted that the martensitic phase on these compounds is ferrimagnetic while, as we have shown, the Cr substitution enhances the ferromagnetic interactions of the martensite phase. This, together with a large thermal hysteresis and low dT_M/dH, hamper the potential of these material for refrigeration applications.

IV. CONCLUSIONS

To summarize, we have successfully produced single-phase $Ni_2Cr_xMn_{1.4-x}In_{0.6}$ samples with Cr substitutions of $x = 0.1$, 0.2, and 0.3 at the Mn site. This substitution shifts the martensitic phase transition towards lower temperatures and enhances the ferromagnetic order of the martensitic phase. We have characterized the adiabatic temperature change ΔT_{ad} for 2 and 6 T field pulses with paying special attention to the irreversibility of the MCE. All samples exhibit large magnetocaloric effects, however, due to the large thermal hysteresis and the weaker field sensitivity of the martensitic transition to the magnetic field with Cr substitution, the effect is irreversible. However, even with the presence of an irreversible window, $Ni_2Cr_{0.1}Mn_{1.3}In_{0.6}$ shows a large magnetocaloric effect. Our results show the effect of element substitution and, consequently, chemically induced pressure, on the magnetic and magnetocaloric properties of Ni-Mn-In-based Heusler alloys.

ACKNOWLEDGMENTS

We acknowledge support from the Würzburg-Dresden Cluster of Excellence on Complexity and Topology in Quantum Matter–*ct.qmat* (EXC 2147, Project No. 390858490), as well as the support of the HLD at HZDR, member of the European Magnetic Field Laboratory (EMFL). P.D. acknowledge support from the Institute for Basic Science under Grant IBS-R027-D1. S.S. thanks the Science and Engineering Research Board of India for financial support through the award of Ramanujan Fellowship (Grant No. SB/S2IRJN-015/2017) and Early Career Research Award (Grant No. ECR/2017/003186). This work was financially supported by the ERC Advanced Grant "TOPMAT" (No. 742068).

[1] J. Liu, T. Gottschall, K. P. Skokov, J. D. Moore, and O. Gutfleisch, Giant magnetocaloric effect driven by structural transitions, Nat. Mater. **11**, 620 (2012).

[2] T. Krenke, E. Duman, M. Acet, E. F. Wassermann, X. Moya, L. Mañosa, and A. Planes, Inverse magnetocaloric effect in ferromagnetic Ni-Mn-Sn alloys, Nat. Mater. **4**, 450 (2005).

[3] A. Aznar, A. Gracia-Condal, A. Planes, P. Lloveras, M. Barrio, J.-L. Tamarit, W. Xiong, D. Cong, C. Popescu, and L. Mañosa, Giant barocaloric effect in all-d-metal Heusler shape memory alloys, Phys. Rev. Materials **3**, 044406 (2019).

[4] R. Kainuma, Y. Imano, W. Ito, Y. Sutou, H. Morito, S. Okamoto, O. Kitakami, K. Oikawa, A. Fujita, T. Kanomata, and K. Ishida, Magnetic-field-induced shape recovery by reverse phase transformation, Nature (London) **439**, 957 (2006).

[5] T. Krenke, E. Duman, M. Acet, E. F. Wassermann, X. Moya, L. Mañosa, A. Planes, E. Suard, and B. Ouladdiaf, Magnetic superelasticity and inverse magnetocaloric effect in Ni-Mn-In, Phys. Rev. B **75**, 104414 (2007).

[6] A. Gracia-Condal, T. Gottschall, L. Pfeuffer, O. Gutfleisch, A. Planes, and L. Mañosa, Multicaloric effects in metamagnetic Heusler Ni-Mn-In under uniaxial stress and magnetic field, Appl. Phys. Rev. **7**, 041406 (2020).

[7] P. Devi, C. Salazar Mejía, M. G. Zavareh, K. K. Dubey, Pallavi Kushwaha, Y. Skourski, C. Felser, M. Nicklas, and Sanjay Singh, Improved magnetostructural and magnetocaloric reversibility in magnetic Ni-Mn-In shape-memory Heusler alloy by optimizing the geometric compatibility condition, Phys. Rev. Materials **3**, 062401(R) (2019).

[8] M. Ghorbani Zavareh, C. Salazar Mejía, A. K. Nayak, Y. Skourski, J. Wosnitza, C. Felser, and M. Nicklas, Direct measurement of the magnetocaloric effect in the Heusler alloy $Ni_{50}Mn_{35}In_{15}$ in pulsed magnetic fields, Appl. Phys. Lett. **106**, 071904 (2015).

[9] P. Devi, M. Ghorbani Zavareh, C. Salazar Mejía, K. Hofmann, B. Albert, C. Felser, M. Nicklas, and Sanjay Singh, Reversible adiabatic temperature change in the shape memory Heusler alloy $Ni_{2.2}Mn_{0.8}Ga$: An effect of structural compatibility, Phys. Rev. Materials **2**, 122401(R) (2018).

[10] K. K. Dubey, P. Devi, A. K. Singh, and S. Singh, Improved crystallographic compatibility and magnetocaloric reversibility in Pt substituted $Ni_2Mn_{1.4}In_{0.6}$ magnetic shape memory Heusler alloy, J. Magn. Magn. Mater. **507**, 166818 (2020).

[11] V. V. Khovaylo, K. P. Skokov, Y. S. Koshkid'ko, V. V. Koledov, V. G. Shavrov, V. D. Buchelnikov, S. V. Taskaev, H. Miki, T. Takagi, and A. N. Vasiliev, Adiabatic temperature change at first-order magnetic phase transitions: $Ni_{2.19}Mn_{0.81}Ga$ as a case study, Phys. Rev. B **78**, 060403(R) (2008).

[12] V. V. Khovaylo, K. P. Skokov, O. Gutfleisch, H. Miki, T. Takagi, T. Kanomata, V. V. Koledov, V. G. Shavrov, G. Wang, E. Palacios, J. Bartolomé, and R. Burriel, Peculiarities of the magnetocaloric properties in Ni-Mn-Sn ferromagnetic shape memory alloys, Phys. Rev. B **81**, 214406 (2010).

[13] V. Basso, C. P. Sasso, K. P. Skokov, O. Gutfleisch, and V. V. Khovaylo, Hysteresis and magnetocaloric effect at the magnetostructural phase transition of Ni-Mn-Ga and Ni-Mn-Co-Sn Heusler alloys, Phys. Rev. B **85**, 014430 (2012).

[14] P. Devi, C. Salazar Mejía, L. Caron, Sanjay Singh, M. Nicklas, and C. Felser, Effect of chemical and hydrostatic pressure on the coupled magnetostructural transition of Ni-Mn-In Heusler alloys, Phys. Rev. Materials **3**, 122401(R) (2019).

[15] Vladimir V. Sokolovskiy, P. Entel, V. D. Buchelnikov, and M. E. Gruner, Achieving large magnetocaloric effects in Co- and Cr-substituted Heusler alloys: Predictions from first-principles and Monte Carlo studies, Phys. Rev. B **91**, 220409(R) (2015).

[16] V. D. Buchelnikov, V. V. Sokolovskiy, O. N. Miroshkina, D. R. Baigutlin, and M. A. Zagrebin, Phase transformations in Ni(Co)-Mn(Cr,C)-(In,Sn) alloys: An ab initio study, Phys. Met. Metallogr. **121**, 202 (2020).

[17] S. Pandey, A. Quetz, A. Aryal, A. U. Saleheen, I. Rodionov, M. Blinov, M. Prudnikova, I. Dubenko, V. Prudnikov, D. Mazumdar, A. Granovsky, S. Stadler, and N. Ali, Effects of the partial substitution of Ni by Cr on the transport, magnetic, and magnetocaloric properties of $Ni_{50}Mn_{37}In_{13}$, AIP Adv. **7**, 056433 (2017).

[18] V. K. Sharma, M. K. Chattopadhyay, S. K. Nath, K. J. S. Sokhey, R. Kumar, P. Tiwari, and S. B. Roy, The effect of substitution of Mn by Fe and Cr on the martensitic transition in the $Ni_{50}Mn_{34}In_{16}$ alloy, J. Phys.: Condens. Matter **22**, 486007 (2010).

[19] H. S. Akkera, I. Singh, and D. Kaur, Room temperature magnetocaloric effect in Ni-Mn-In-Cr ferromagnetic shape memory alloy thin films, J. Magn. Magn. Mater. **424**, 194 (2017).

[20] V. K. Sharma, M. K. Chattopadhyay, L. S. Sharath, and S. B. Roy, Elevating the temperature regime of the large magnetocaloric effect in a Ni-Mn-In alloy towards room temperature, J. Phys. D: Appl. Phys. **44**, 145002 (2011).

[21] V. Sanchez-Alarcos, V. Recarte, J. I. Perez-Landazabal, J. R. Chapelon, and J. A. Rodriguez-Velamazan, Structural and magnetic properties of Cr-doped Ni-Mn-In metamagnetic shape memory alloys, J. Phys. D: Appl. Phys. **44**, 395001 (2011).

[22] S. Singh, P. Kushwaha, F. Scheibel, H. P. Liermann, S. R. Barman, M. Acet, C. Felser, and D. Pandey, Residual stress induced stabilization of martensite phase and its effect on the magnetostructural transition in Mn-rich Ni-Mn-In/Ga magnetic shape memory alloys, Phys. Rev. B **92**, 020105(R) (2015).

[23] See Supplemental Material at http://link.aps.org/supplemental/10.1103/PhysRevMaterials.5.104406 for extra information about sample homogeneity, magnetization curves at the martensite and austenite phases for all samples, and information about a sample with higher Cr concentration, $x = 0.4$.

[24] S. Aksoy, M. Acet, P. P. Deen, L. Mañosa, and A. Planes, Magnetic correlations in martensitic Ni-Mn-based Heusler shape-memory alloys: Neutron polarization analysis, Phys. Rev. B **79**, 212401 (2009).

[25] M. Khan, I. Dubenko, S. Stadler, J. Jung, S. S. Stoyko, A. Mar, A. Quetz, T. Samanta, N. Ali, and K. H. Chow, Enhancement of ferromagnetism by Cr doping in Ni-Mn-Cr-Sb Heusler alloys, Appl. Phys. Lett. **102**, 112402 (2013).

[26] A. Taubel, T. Gottschall, M. Fries, S. Riegg, C. Soon, K. P. Skokov, and O. Gutfleisch, A comparative study on the magnetocaloric properties of Ni-Mn-X(-Co) Heusler alloys, Phys. Status Solidi B **255**, 1700331 (2018).

[27] S. Kustov, I. Golovin, M. L. Corro, and E. Cesari, Isothermal martensitic transformation in metamagnetic shape memory alloys, J. Appl. Phys. **107**, 053525 (2010).

[28] E. Cesari, D. Salas, and S. Kustov, Entropy changes in ferromagnetic shape memory alloys, Mater. Sci. Forum. **684**, 49 (2011).

[29] T. Kihara, X. Xu, W. Ito, R. Kainuma, and M. Tokunaga, Direct measurements of inverse magnetocaloric effects in metamagnetic shape-memory alloy NiCoMnIn, Phys. Rev. B **90**, 214409 (2014).

[30] C. Salazar Mejía, M. Ghorbani Zavareh, A. K. Nayak, Y. Skourski, J. Wosnitza, C. Felser, and M. Nicklas, Pulsed high-magnetic-field experiments: New insights into the magnetocaloric effect in Ni-Mn-In Heusler alloys, J. Appl. Phys. **117**, 17E710 (2015).

[31] T. Gottschall, K. P. Skokov, D. Benke, M. E. Gruner, and O. Gutfleisch, Contradictory role of the magnetic contribution in inverse magnetocaloric Heusler materials, Phys. Rev. B **93**, 184431 (2016).

[32] L. Pfeuffer, T. Gottschall, T. Faske, A. Taubel, F. Scheibel, A. Y. Karpenkov, S. Ener, K. P. Skokov, and O. Gutfleisch, Influence of the martensitic transformation kinetics on the magnetocaloric effect in Ni-Mn-In, Phys. Rev. Materials **4**, 111401(R) (2020).

[33] N. T. Trung, J. C. P. Klaasse, O. Tegus, D. T. C. Thanh, K. H. J. Buschow, and E. Bruck, Determination of adiabatic temperature change in MnFe(P,Ge) compounds with pulse-field method, J. Phys. D: Appl. Phys. **43**, 015002 (2010).

[34] C. Salazar-Mejía, V. Kumar, C. Felser, Y. Skourski, J. Wosnitza, and A. K. Nayak, Measurement-Protocol Dependence of the Magnetocaloric Effect in Ni-Co-Mn-Sb Heusler Alloys, Phys. Rev. Appl. **11**, 054006 (2019).

[35] T. Gottschall, K. P. Skokov, R. Burriel, and O. Gutfleisch, On the S(T) diagram of magnetocaloric materials with first-order transition: Kinetic and cyclic effects of Heusler alloys, Acta Mater. **107**, 1 (2016).